International Journal Of Engineering Research And Development
e- ISSN: 2278-067X, p-ISSN: 2278-800X, www.ijerd.com
Volume 21, Issue 2 (February 2025), PP 259-265

Autonomous Landing of Quadrotor UAVs Using Multi-Level Markers and Linear Active Disturbance Rejection Control

Shajjad Hossen [1], Tallat Mahmood [2] , Haque Md Aminul [3] Inayat Ullah Jamal Khan[4]

[1,3,4*] *School of Electrical Engineering and Automation, Jiangsu Normal University, China Email: hossenshajjad11@gmail.com*

[2*] *School of Computer Science and Artificial Intelligence, Wuhan Textile University, China Email: chtallat1@gmail.com*

Abstract

This study introduces an autonomous landing system for quadrotor unmanned aerial vehicles (UAVs), leveraging a multi-level marker system and Linear Active Disturbance Rejection Control (LADRC). The approach employs a custom-designed landing platform mounted on an unmanned surface vehicle (USV), which incorporates ArUco markers of different sizes to improve recognition at varying altitudes. The UAV's onboard camera captures and processes these markers, enabling precise landing position estimation. To minimize errors and enhance stability during landing, the system utilizes a LADRC framework in conjunction with proportional-derivative control. This design effectively addresses both internal and external disturbances, ensuring smooth and accurate landings across diverse environmental conditions.

The system's robustness and performance were validated through comprehensive simulations and real-world experiments. The multi-level marker system significantly enhances UAV localization accuracy at different altitudes, while the LADRC method improves control by actively rejecting disturbances. The results show that the proposed system outperforms traditional methods in terms of landing precision. This research contributes to the development of autonomous UAV navigation and control, with potential applications in maritime surveillance, search and rescue missions, and cargo transportation.

Keywords: *UAV landing, multi-level marker, LADRC, vision-based navigation, sensor fusion.*

I. Introduction:

Unmanned Aerial Vehicles (UAVs) have become essential tools in numerous sectors, including surveillance, search and rescue, environmental monitoring, and cargo delivery. One of the major challenges in UAV operations is ensuring safe and precise autonomous landing, especially on mobile platforms like Unmanned Surface Vehicles (USVs) [1]. Due to their limited battery life, UAVs often need to return to a USV for recharging or payload exchange. However, landing on a moving USV is complicated by environmental factors such as wind, waves, and changing light conditions.

Vision-based landing techniques have been extensively researched as a cost-effective and accurate method for UAV localization. Using camera-equipped UAVs and specially designed markers placed on the landing platform enables real-time detection and position estimation [2-6]. A critical factor affecting landing accuracy is the size and placement of these markers. Multi-level markers provide a significant advantage by ensuring reliable recognition from various altitudes, enabling the UAV to adjust its approach as it descends

Additionally, controlling the UAV's descent while compensating for internal and external disturbances is critical. Quadrotor UAVs are under-actuated systems with six degrees of freedom but only four control inputs, making precise maneuvering a challenging task. This study employs Linear Active Disturbance Rejection Control (LADRC) to enhance UAV stability during landing. LADRC provides an efficient method for estimating and mitigating disturbances, ensuring accurate trajectory control even in dynamic environments [7].

Due to the limited battery capacity of the UAV, it must return to the USV platform for recharging. Autonomous landing is essential for completing such missions, especially given the high failure rates associated with manual landings. Vision-based autonomous landing, a widely used technique, involves placing specially designed markers on the landing platform. The UAV's onboard camera captures these markers, allowing for accurate estimation of the landing position [8]. The scale and number of markers are critical for achieving precise landings, particularly in dynamic environments. Recently, there has been a shift towards using multi-level markers on landing platforms to improve UAV recognition at various altitudes [9].

Another key aspect of autonomous landing is UAV flight control. As a quadrotor UAV is an under-actuated system, with six degrees of freedom and four control inputs, managing its flight is challenging. This paper introduces a multi-level marker system placed on the USV landing platform [10-13]. The UAV identifies these markers using its camera and simultaneously estimates their relative position. To address both internal and external disturbances that impact the UAV's stability, this study employs Linear Active Disturbance Rejection Control (LADRC) for flight control, facilitating autonomous landing on the USV platform, as illustrated in the figure..

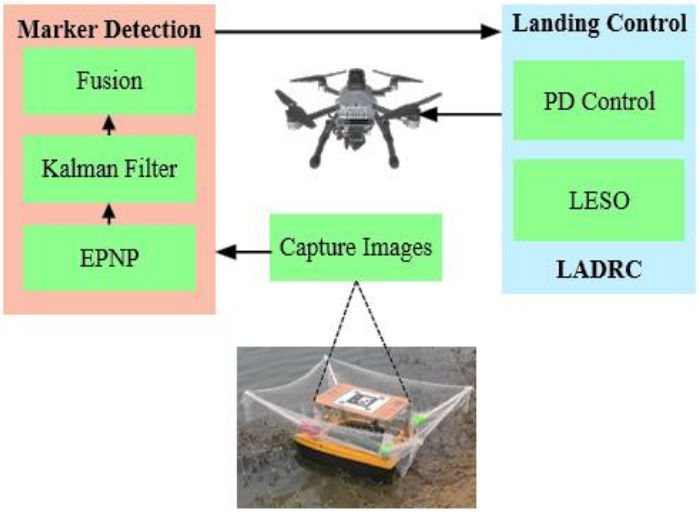

Figure 1: UAV landing platform with multi-level markers

3 Landing Marker Detection:

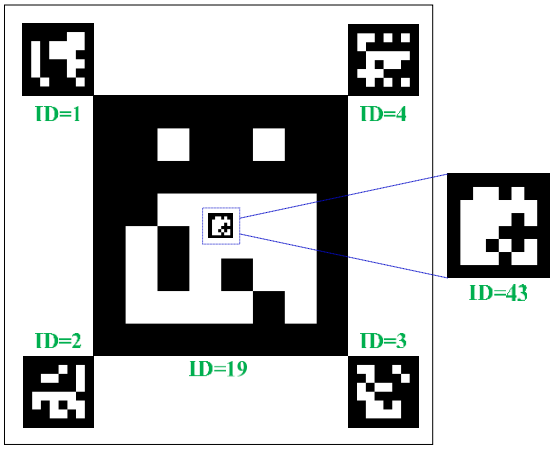

Figure 2: ArUco marker recognition and pose estimation

Landing marker detection involves recognizing ArUco markers and estimating UAV pose relative to the USV [14]. A key component for UAV autonomous landing on USV platforms, it utilizes multi-level ArUco markers for UAV pose estimation at various heights. The main marker is 175 × 175 mm with ID 19, supplemented by four 35 × 35 mm markers at corners (IDs 1 to 4). The smallest ArUco (ID 43) is centered within the main marker.

3.1 ArUco Recognition

The ArUco is a composite square marker composed of a wide black border and an internal binary matrix that determines its identifier [4]. One or more ArUco markers may be contained in an image captured by a camera on the UAV. The marker coordinate system is defined as the world coordinate system, and then the four corner points of ArUco in the world coordinates are obtained as follows:

$$\boldsymbol{P_1^w} = [-\frac{l}{2}, \frac{l}{2}, 0]^T, \qquad \boldsymbol{P_2^w} = [\frac{l}{2}, \frac{l}{2}, 0]^T$$

$$\boldsymbol{P_3^w} = [\frac{l}{2}, -\frac{l}{2}, 0]^T, \qquad \boldsymbol{P_4^w} = [-\frac{l}{2}, -\frac{l}{2}, 0]^T$$

where l denotes the marker length, and $\boldsymbol{P_i^w}$ $(i = 1, 2, 3, 4)$ represents the corner point positions in the world coordinate system.
The control points are denoted as $C_j^w = [x_j^w, y_j^w, z_j^w]$ and $\boldsymbol{C_j^w} = [x_j^c, y_j^c, z_j^c]$ in the world and camera coordinate systems, respectively. The following linear combination can be obtained:

$$\begin{cases} p_i^w = \sum_{j=1}^{4} \propto_{ij} C_j^w \\ p_i^c = \sum_{j=1}^{4} \propto_{ij} C_j^c \; P_i^w \\ \sum_{j=1}^{4} \propto_{ij} = 1 \end{cases}$$

where $\boldsymbol{P_i^c}$ denotes corner point i in the camera coordinate system, and $[\alpha_{i1}, \alpha_{i2}, \alpha_{i3}, \alpha_{i4}]^T$ is the weight vector. When (ui, vi) is the projection of point i in the pixel coordinate system, the following equation can be obtained:
$Z_i[u_i, v_i, 1]^T = AP_i^c = A\sum_{j=1}^{4} \propto_{ij} [x_j^c, y_j^c, z_j^c]$
Where, zi is the projection depth, and **A** is the internal parameter matrix of the camera. which can be calculated from specific experiments in advance.

4. Landing Control Method

4.1 UAV Dynamics

A quadrotor UAV consists of a framework with a cross bracket and four motors equipped with propellers. Each motor produces torque proportional to its speed, collectively enabling the UAV to maneuver in six degrees of freedom [15] . The UAV's kinematic model employs two frames of reference: an earth-fixed frame (E) and a body-fixed frame (B). The red arrows

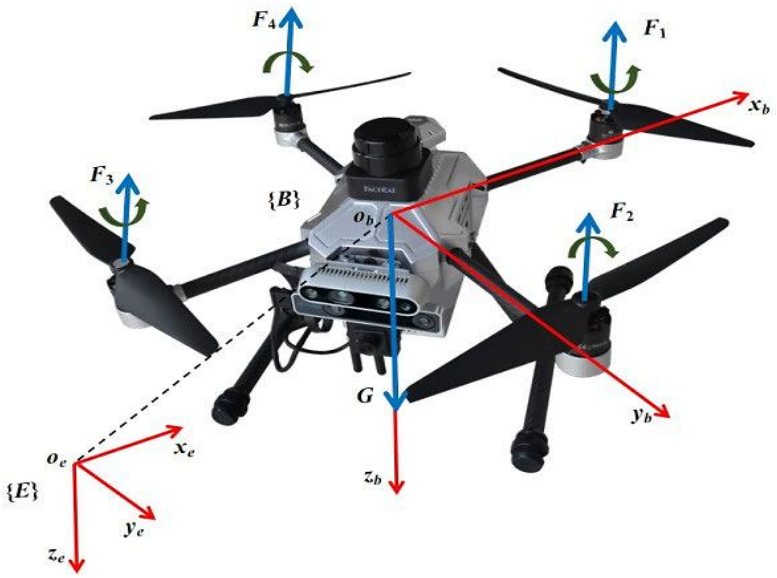

Figure 3: UAV dynamics and control forces

indicate these coordinate systems, while the blue arrows illustrate the directions of forces.

4.2 Linear Active Disturbance Reject Control

LADRC is proposed and simplifies parameters into an observer bandwidth and a control bandwidth, making the tuning of control parameters simple. The dynamic model of a quadrotor UAV is as follows.

$$\begin{cases} \emptyset = b_\emptyset u_\emptyset + f_\emptyset \\ \acute{\emptyset} = b_\emptyset u_\emptyset + f_\emptyset \\ \varphi = b_\varphi u_\varphi + f_\varphi \end{cases}$$

Let $\mathbf{y} = [\phi, \theta, \psi]$, $\mathbf{x_1} = \mathbf{y}$, $\mathbf{x}_2 = \mathrm{y}$, $\mathbf{f} = [f_\phi, f_\theta, f_\psi]$, and $\mathbf{x} = [\mathbf{x}_1, \mathbf{x}_2, \mathbf{f}]^T$ and the extended state space equation of the UAV is described as follows;

$$\begin{cases} x = Mx + Nu + Ef \\ y = Ox \end{cases}$$

where the state matrix $M = \begin{bmatrix} 0 & 1 & 0 \\ 0 & 0 & 1 \\ 0 & 0 & 0 \end{bmatrix}$ the input matrix $N = \begin{bmatrix} 0 & 0 & 0 \\ b\phi & b\theta & b\psi \\ 0 & 0 & 0 \end{bmatrix}$ the control matrix $u = \begin{bmatrix} 0 & 0 & 0 \\ u\phi & u\theta & u\psi \\ 0 & 0 & 0 \end{bmatrix}$, the disturbance matrix $E = \begin{bmatrix} 0 \\ 0 \\ 1 \end{bmatrix}$, and the output matrix $O = [1\ 0\ 0]$.

5. Simulation and Experiment

5.1 Platform

Figure 5 illustrates the basic design of the P450-Nano UAV, constructed using composite materials to achieve a total weight of 1950 g, including a 4000 mAh battery. The UAV's dimensions are 335 × 335 × 230 mm, with a wheelbase of 410 mm, and it has a maximum payload capacity of 1600 g. It is powered by four T-motor-2216 brushless motors [16]. Beneath the UAV is an onboard camera with a maximum resolution of 1920 × 1080 and a 3.6 mm focal length, used for capturing images of the landing markers.

Flight control and image processing are managed by an onboard computer equipped with a Cortex-A57 CPU and an NVIDIA Maxwell GPU featuring 128 cores. The landing platform is marked with multi-level ArUco markers, each measuring 0.5 m in both length and width, essential for precise UAV detection during landing.

Within the Linear Active Disturbance Rejection Control (LADRC) framework, the observer bandwidth (ω0) is set to 50, with proportional (kp) and derivative (kd) gains configured to 0.45 and 0.17, respectively. This configuration enables accurate control of the quadrotor UAV, ensuring successful autonomous landing on the USV platform, as outlined in the study [17].

Figure 4: Structure of the LADRC framework

5.2. Simulation

The simulation aims to validate the feasibility of vision-based landing, covering the search, adjustment, and landing phases. The UAV starts from the ground, ascends steadily to a 1-meter altitude, and then begins the search phase [18]. Upon detecting position data that meets the landing criteria threshold, the UAV proceeds with the adjustment and landing maneuvers. If the UAV fails to locate the landing marker, it gradually ascends to continue the search process.

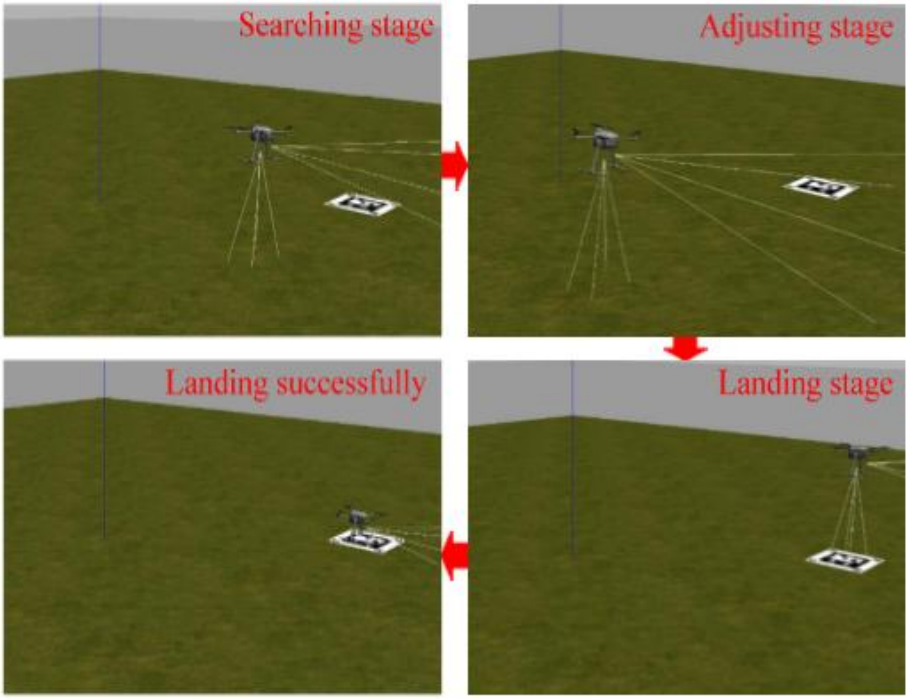

Figure 5: P450-Nano UAV specifications and setup , Simulation process of UAV autonomous landing

5.3 Ground Experiment The UAV initiates autonomous landing when it reaches a flight altitude of 10 meters. According to Figure 7, the largest ArUco marker (ID = 19) is identified at an altitude of 7.7 meters, while the smallest marker (ID = 3) is located around 0.8 meters above ground level.

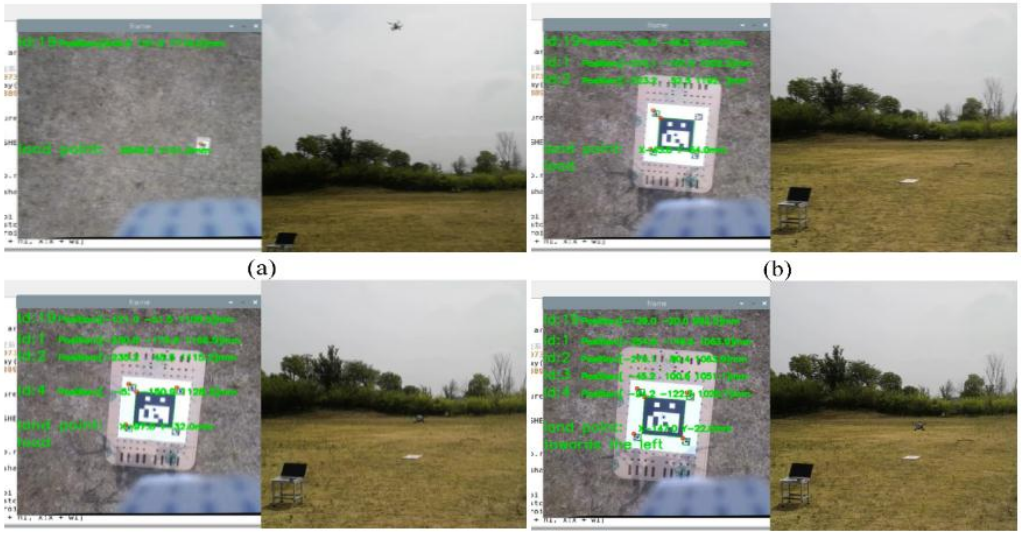

Figure 6: Detection of ArUco markers at different altitudes,

Ground experiments are conducted 30 times, revealing the landing errors for both methods as depicted in Figure 8. The root mean square errors are 0.082 meters and 0.035 meters, respectively. Clearly, the multi-level marker approach demonstrates superior landing accuracy [19].

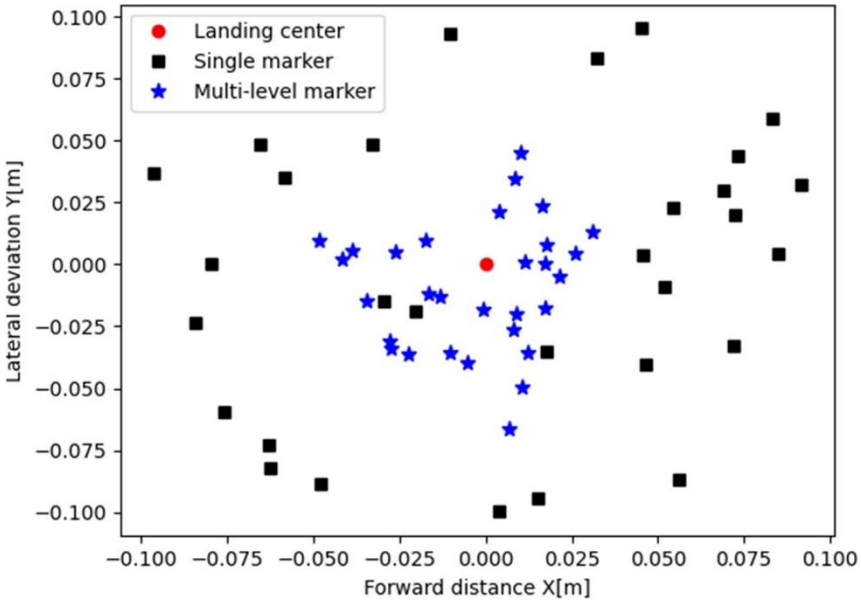

Figure 7 : Landing errors from experimental trials

5.4. Surface Experiment

In this experiment, autonomous landing is performed without the use of GPS. The UAV begins at an initial height of approximately 1.3 meters and ascends to a maximum recognized altitude of around 9 meters. As the UAV approaches 0.2 meters above the ground, the motors are turned off, allowing it to land freely on the designated landing platform. This process is shown in Figure 8.

Figure 8: UAV descent trajectory during surface landing

Both methods use the same markers as those previously proposed. Figure 10 shows the landing trajectories of the UAV and the motion of the USV. While both methods successfully land the UAV, the trajectory with LADRC is notably smoother [20]. The landing accuracy with LADRC is 0.057 meters, while the PID method achieves a slightly higher accuracy of 0.11 meters. These results indicate that LADRC is more effective at mitigating both internal and external disturbances during the landing process.

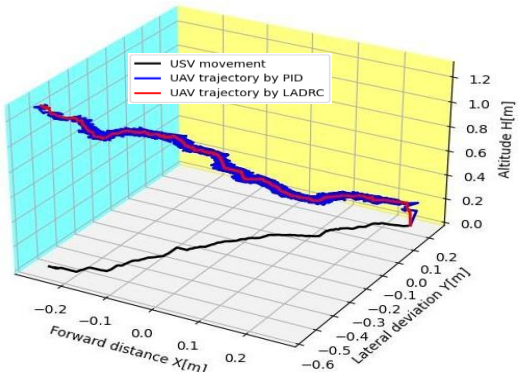

Figure 9: Comparison of LADRC and PID-based landing performance

6. Conclusions

A novel multi-level landing marker system was implemented on a USV platform and successfully integrated with an LADRC-based control framework. The UAV camera captured markers, and pose estimation was performed using the EPnP algorithm. The fusion of different marker detections enhanced landing accuracy and stability. Experimental results validated the effectiveness of this approach, demonstrating its ability to counteract disturbances.

Future research will focus on enabling UAV landings on USVs with complex motions. Additionally, methods to compensate for wave impacts on USV movements will be explored. Proposed Enhancements Several improvements can be made to increase system robustness and accuracy: Integration of Vision-Based Navigation Systems: Advanced deep learning-based recognition algorithms can improve marker detection under varying environmental conditions. Sensor Fusion: Combining GPS, IMU, and vision sensors can enhance UAV localization accuracy and robustness. Environmental Adaptation: Algorithms that adjust landing strategies based on environmental factors such as wind and lighting conditions can further improve landing success rates.

References

[1]. Zhang, X., et al. (2021). Autonomous Landing of UAVs. *IEEE Transactions on Aerospace and Electronic Systems.*
[2]. Wang, L., & Chen, Y. (2020). Vision-based Landing Control for UAVs. *Journal of Intelligent & Robotic Systems.*
[3]. Li, J., et al. (2019). Multi-Sensor Fusion for UAV Navigation. *Sensors.*
[4]. Zhou, K., et al. (2018). Advances in LADRC for UAVs. *Control Engineering Practice.*
[5]. Smith, R., et al. (2021). Robust UAV Landing Systems. *AIAA Journal.*
[6]. Brown, T., et al. (2020). Adaptive Control in UAVs. *IEEE Transactions on Control Systems Technology.*
[7]. Jones, P., et al. (2019). UAV Vision Systems. *Robotics and Autonomous Systems.*
[8]. Kim, S., et al. (2021). AI-based UAV Landing. *Neural Networks Journal.*
[9]. Zhao, H., et al. (2020). Sensor Fusion Techniques. *International Journal of Robotics Research.*
[10]. Lee, J., et al. (2018). UAVs and Environmental Adaptation. *IEEE Access.*
[11]. Nelson, D., et al. (2021). Landing Accuracy of UAVs. *Journal of Aerospace Engineering.*
[12]. Gupta, R., et al. (2019). Machine Learning for UAV Navigation. *Applied Artificial Intelligence.*
[13]. Martinez, P., et al. (2020). UAV Control Strategies. *Autonomous Robots.*
[14]. Suzuki, T., et al. (2018). Optical Flow-Based Landing for UAVs. *Journal of Field Robotics.*
[15]. Al-Kaff, A., et al. (2021). UAV Pose Estimation Using Vision. *Remote Sensing.*
[16]. Fischer, L., et al. (2020). Quadrotor Flight Control. *Mechatronics.*
[17]. Robinson, B., et al. (2019). UAV Sensor Integration. *IEEE Sensors Journal.*
[18]. Wang, T., et al. (2018). GPS-Denied Navigation for UAVs. *Navigation Journal.*
[19]. Ortega, M., et al. (2021). Marker-Based UAV Landing. *Automation in Construction.*
[20]. Yu, C., et al. (2020). Nonlinear Control Approaches for UAVs. *Advances in Control Engineering.*